Radiative Corrections to Symmetric Pair Production

B. HULD*†
Physics Department, Harvard University, Cambridge, Massachusetts
(Received 20 November 1967; revised manuscript received 25 January 1968)

The radiative corrections to symmetric pair production are calculated to a high degree of accuracy. The matrix element squared for the hard-photon correction is expressed approximately in a simple form which, for symmetric pair production, describes the corresponding radiative correction to better than 1%. This approximation improves on the often-used peaking approximation. The results are useful also for calculating radiative corrections to bremsstrahlung and trident production.

INTRODUCTION

RECENT experiments on symmetric wide-angle pair production have attempted to test quantum electrodynamics at high energies.[1-3] Pair production at symmetry is particularly well suited for such a purpose because the cross section can be shown to be dominated by purely electromagnetic effects, namely, the basic Bethe-Heitler mechanism and its radiative corrections.[4,5] The Bethe-Heitler cross section is well known, but a thorough calculation of the radiative corrections, especially the hard-photon radiative correction, is lacking.

The Feynman diagrams for pair production via the Bethe-Heitler mechanism are given in Fig. 1. The cross section corresponding to these diagrams was first calculated by the authors whose names are now associated with it.[6] Bjorken, Drell, and Frautschi extended the original calculation by including nuclear recoil and elastic form factors.[5] Drell and Walecka completed the calculation by including the mass of the electron and the general form factors.[7] In Sec. I of this paper we will discuss the Bethe-Heitler cross section with particular reference to its behavior in the region of experimental interest.

The experiments on symmetric wide-angle pair production have all been performed in approximately the same manner. An incident bremsstrahlung beam strikes a carbon target to produce, among other things, electron-positron pairs. The four-momenta p_- and p_+ of the electron and positron are determined completely by two spectrometers located symmetrically, one on either side of the forward direction defined as the direction of the incoming photon beam. The center of acceptance of the spectrometers is the point of complete symmetry where the energies of the two particles and the angles they make with the forward direction are equal. Knowing the momenta of the electron and positron and assuming elastic scattering, one can calculate the energy k of the photon producing the event. This energy is taken typically to be 4/5 of the maximum energy $k_{\max}$ of the photon spectrum, thereby limiting somewhat the number of inelastic processes possible. Nonetheless, the inelastic events are not negligible. In particular, for a 5-BeV bremsstrahlung beam it is possible to radiate an undetected "hard" photon of energy up to 1 BeV. It is this fact which necessitates a thorough treatment of the radiative correction due to the emission of real photons.

The Feynman diagrams for the radiative corrections to order α^4 are given in Figs. 2 and 3. The radiative corrections of Fig. 2 will be referred to as the "virtual photon correction" and those of Fig. 3 as the "real photon correction." In addition, it is convenient to divide the real photon correction into the "soft"-photon and the "hard"-photon correction. The soft-photon correction is due to the emission of photons of energy less than δ, where $\delta \ll m$ (m is the mass of the electron), and the hard-photon correction is then the remainder of the real photon correction. The reason for this division is that the soft-photon correction is infrared

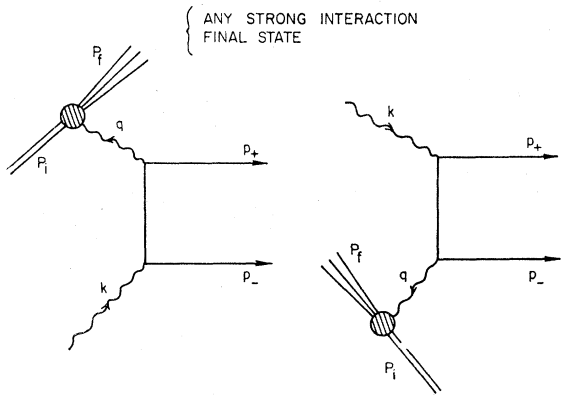

FIG. 1. The Bethe-Heitler diagrams for pair production.

* This work was supported by the U. S. Atomic Energy Commission under Contract AT(30-1)2752.
† This paper is based in part on material submitted to Harvard University in partial fulfillment of the requirements for the Doctor of Philosophy degree.

[1] R. B. Blumenthal, D. C. Ehn, W. L. Faissler, P. M. Joseph, L. J. Lanzerotti, F. M. Pipkin, and D. G. Stairs, Phys. Rev. 144, 1199 (1966).
[2] E. Eisenhandler, J. Feigenbaum, N. Mistry, P. Mostek, D. Rust, A. Silverman, C. Sinclair, and R. Talman, Phys. Rev. Letters 18, 425 (1967).
[3] J. G. Asbury, W. K. Bertram, U. Becker, P. Joos, M. Rohde, A. J. S. Smith, S. Friedlander, C. Jordan, and C. C. Ting, Phys. Rev. Letters 18, 65 (1967); Phys. Rev. 161, 1344 (1967).
[4] S. D. Drell, Ann. Phys. (N. Y.) 4, 75 (1958).
[5] J. D. Bjorken, S. D. Drell, and S. C. Frautschi, Phys. Rev. 112, 1409 (1958).
[6] H. Bethe and W. Heitler, Proc. Roy. Soc. (London) 146, 83 (1934).
[7] S. D. Drell and J. D. Walecka, Ann. Phys. (N. Y.) 28, 18 (1964).

TABLE I. Definitions of symbols for pair production.

$p_+=(E_+,\mathbf{p}_+)$ = four-momentum of positron.
$p_-=(E_-,\mathbf{p}_-)$ = four-momentum of electron.
$k=(k,\mathbf{k})$ = four-momentum of incident photon.
$k_{\max}$ = maximum photon energy of bremsstrahlung beam.
$\Delta E=k_{\max}-E_+-E_-$.
e = polarization vector of incident photon.
$l=(l_0,\mathbf{l})$ = four-momentum of radiated photon.
e_l = polarization vector of radiated photon.
$P_i=(E_i,\mathbf{P}_i)$ = four-momentum of initial nucleus.
$P_f=(E_f,\mathbf{P}_f)$ = four-momentum of final nuclear state.
$q=k-p_+-p_-$ = momentum transfer to the nucleus.
$R=P_i+P_f$.
$\Delta=p_--p_+$.
$Q=p_-+p_+$; Q^2 is the mass of the electron-positron final state.
θ_+ = angle between $\mathbf{p}_+$ and $\mathbf{k}$.
θ_- = angle between $\mathbf{p}_-$ and $\mathbf{k}$.
φ = angle between the $(\mathbf{p}_+,\mathbf{k})$ plane and the $(\mathbf{p}_-,\mathbf{k})$ plane.
$M_i=|P_i^2|^{1/2}$ = mass of initial nucleus.
$M_f=|P_f^2|^{1/2}$ = mass of final nuclear state.
m = mass of electron.
$\beta_\pm=2k\cdot p_\pm$; $l_\pm=2l\cdot p_\pm$.
$\theta=\frac{1}{2}(\theta_++\theta_-)$; $E=\frac{1}{2}(E_++E_-)$.
$a=(\theta_+-\theta_-)/(\theta_++\theta_-)$; $\epsilon=(E_+-E_-)/(E_++E_-)$.

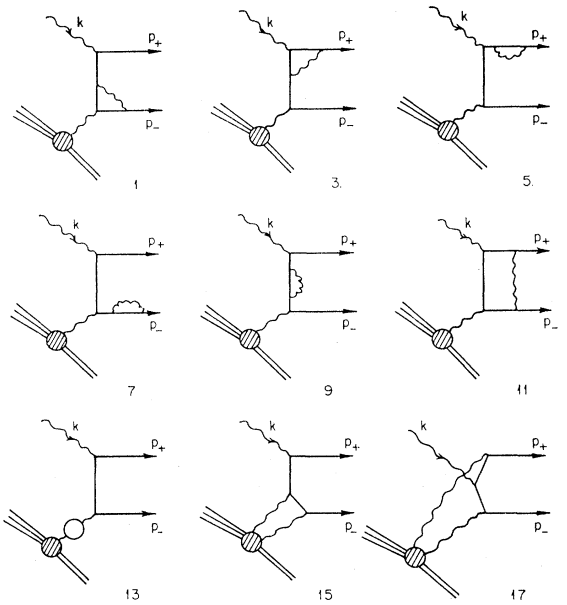

FIG. 2. Feynman diagrams for the virtual photon correction. Each even-numbered diagram (not shown) can be obtained by exchanging p_+ and p_- on the preceding odd-numbered diagram.

divergent. To deal with this problem we follow Yennie, Frautschi, and Suura.[8] We give the photon a small mass λ and show that the terms divergent as $\lambda\to 0$ cancel against similar terms in the virtual photon correction.

Bjorken, Drell, and Frautschi[5] have calculated approximately the radiative correction to symmetric pair production. Their result is

$$d\sigma_{\mathrm{BH}}{}^{\mathrm{rad}}(\mathrm{BDF})=-\frac{\alpha}{\pi}\ln\frac{2p_+\cdot p_-}{m^2}\left[\frac{13}{6}+\ln\frac{(\Delta E)^2}{E^2}\right]d\sigma_{\mathrm{BH}}, \quad (1)$$

where $\Delta E=k_{\max}-2E$, $E=E_+=E_-$, and $d\sigma_{\mathrm{BH}}$ is the Bethe-Heitler differential cross section. (Definitions of symbols are given also in Table I.) In this calculation only the leading logarithmic terms were considered and, more seriously, of the real photon correction only the soft-photon correction was included. (That is, $\delta=\Delta E$ even though the calculation is performed assuming the emitted photon to be soft.) The calculation has been verified by others to this approximation.[9,10] An attempt has been made to calculate the hard-photon correction exactly, but the result is so complicated that it is not useful to experimentalists without further extensive numerical calculations.[11] Others have attempted to calculate roughly the dominant contribution from the hard-photon correction, but, aside from demonstrating the unreliability of the soft-photon approximation, the results have been inconclusive.[12,13] The virtual correction to bremsstrahlung, which is closely related to pair production, has been calculated in great detail, but for configurations not applicable to our case.[14]

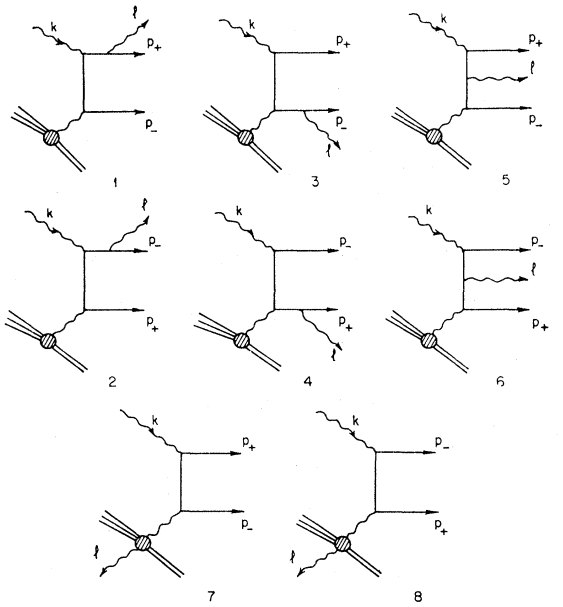

FIG. 3. Feynman diagrams for the real photon correction.

[8] D. R. Yennie, S. C. Frautschi, and H. Suura, Ann. Phys. (N. Y.) **13**, 379 (1961).
[9] P. I. Formin, Zh. Eksperim. i Teor. Fiz. **35**, 707 (1958) [English transl.: Soviet Phys.—JETP **8**, 491 (1959)].
[10] S. Ya. Guzenko and P. I. Formin, Zh. Eksperim. i Teor. Fiz. **38**, 513 (1960) [English transl.: Soviet Phys.—JETP **11**, 372 (1960)].
[11] N. F. Nelipa, Dokl. Akad. Nauk SSSR **148**, 68 (1963) [English transl.: Soviet Phys.—Doklady **8**, 31 (1963)].
[12] E. L. Lomon, Phys. Letters **21**, 555 (1966).
[13] E. Ferrari and P. G. Thurnauer, Nuovo Cimento **45A**, 752 (1966).
[14] A. N. Mitra, P. Narayanaswamy, and L. K. Pande, Nucl. Phys. **10**, 629 (1959).

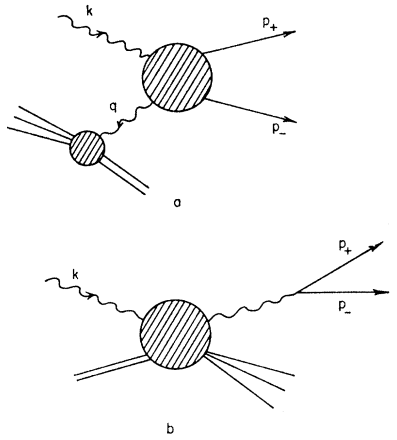

FIG. 4. (a) General Bethe-Heitler-type diagram. (b) General Compton-type diagram.

Both the virtual and real photon corrections have been calculated here, assuming only that the mass of the electron is small compared to other invariants in the problem. The general result for the virtual photon correction is somewhat unwieldy, but when we specialize to the case of symmetric pair production the answer becomes quite simple. The general result for the real photon correction can, on the other hand, be expressed in a surprisingly simple form. This result is the most interesting contribution of this paper and encourages the hope that similarly simple answers may be derived for other scattering problems. In Sec. II of the paper we discuss the virtual photon correction and in Sec. III the real photon correction. In the final section we give the total result with a discussion of its behavior.

As mentioned above, pair production at symmetry is particularly well suited for testing quantum electrodynamics. In order to test the theory, it is necessary to separate electromagnetic and strong-interaction effects since at present there is no adequate theory of strong interactions. In the Bethe-Heitler diagrams the one-photon exchange with the nucleus ensures that the strong-interaction effects can be included in form factors depending only on the momentum transfer to the nucleus q_μ.[7] (More exactly on q^2 and q_0.) These form factors can be measured experimentally from electron-nucleus scattering. In addition, pair production at symmetry minimizes the momentum transfer to the nucleus and hence the effect of form factors.

For pairs produced via the other basic process, the Compton mechanism of Fig. 4(b), no similar separability of electromagnetic and strong interactions is possible. However, by an argument first used by Bjorken, Drell, and Frautschi,[5] it can be shown that the interference of the Compton-type diagram with the Bethe-Heitler diagrams does not contribute to symmetric pair production. Consider first the photon-electron-positron vertex of the Compton-type diagram Fig. 4(b). Applying charge conjugation to the vertex interchanges the electron and positron, or $p_+ \leftrightarrow p_-$, while the photon goes into minus itself. Hence the amplitude for electron-positron pairs produced via the Compton mechanism must be antisymmetric under the exchange $p_+ \leftrightarrow p_-$. Now consider the diagram Fig. 4(a) which includes the Bethe-Heitler diagrams and all the virtual photon radiative corrections involving a one-photon exchange with the nucleus. The relevant vertex is now a photon-photon—electron-positron vertex and hence the amplitude for pairs produced via this process is symmetric under the exchange $p_+ \leftrightarrow p_-$. The interference between the two amplitudes is then antisymmetric in $p_+ \leftrightarrow p_-$ and does not contribute to symmetric pair production. The Compton amplitude squared is not considered here. It has been shown elsewhere to be small except when the mass of the lepton pair is close to the ρ-meson mass.[5,15]

Applying the same argument to the radiative corrections of Fig. 2, it is clear that the interference of the two-photon-exchange diagrams (Figs. 2–15 to 2–18) with the Bethe-Heitler diagrams does not contribute to symmetric pair production. These diagrams squared are of order α^5 and not considered here. Similarly, the interference of diagrams Fig. 3–7 and Fig. 3–8 with the remaining diagrams of Fig. 3 does not contribute to symmetric pair production. Diagrams Fig. 3–7 and Fig. 3–8 squared are included in the experimental form factors as we will show below. Thus there is a complete separability of electromagnetic and strong-interaction effects for these radiative corrections to symmetric pair production.[16] In practice these arguments are not very important because the terms which have been shown rigorously not to contribute to symmetric pair production are actually very small for any pair production with small momentum transfer to the nucleus.[17]

The strong-interaction effects are included in form factors which for any given target must be measured by performing electron scattering experiments with that same target. Before the form factors can be extracted from such an experiment, it is necessary to subtract radiative corrections from the experimental cross section. The diagrams for the basic scattering process and its radiative corrections are given in Fig. 5. Suppose the scattering experiment is performed both with electrons and with positrons in otherwise identical configurations and the relevant cross section defined as the average of the two. Now notice in Fig. 5 that diagram (1) changes sign depending on whether the lepton is an electron or a positron but diagram (6) does not. Then the interference between diagrams (1) and (6) does not contribute to the average cross section. Similarly, the interference between diagram (9) and diagrams (7) and (8) does not contribute to the average

[15] S. M. Berman and S. D. Drell, Phys. Rev. 133, B791 (1964).
[16] More generally the arguments apply to experiments in any configuration where symmetry is inforced by reversing magnet currents halfway through the data taking.
[17] B. Huld, thesis, Harvard University, 1967 (unpublished).

cross section. The form factors are found by comparing the experimental cross section with the theoretical one calculated from the diagrams of Fig. 5 *not* including diagrams (6) and (9). Diagram (9) squared then contributes to the form factors. With this definition of the experimental form factors and the above arguments, we are justified rigorously in ignoring diagrams Fig. 2–15 to Fig. 2–18, Fig. 3–7, and Fig. 3–8 for symmetric pair production. Again, we stress that the arguments here have more theoretical than practical interest because the ignored terms are small for pair production at small momentum transfer. Similarly, the difference between electron and positron nuclear scattering at small momentum transfer is small.[18]

The conventions used in this paper are similar to those used by Bjorken and Drell.[19] The units $\hbar=c=1$ and $e^2/4\pi=\alpha$ are used. The relativistic notation is such that $a\cdot b=a_0b_0-\mathbf{a}\cdot\mathbf{b}$, and $\gamma_\mu\gamma_\nu+\gamma_\nu\gamma_\mu=2g_{\mu\nu}$, where $g_{00}=1$, $g_{11}=g_{22}=g_{33}=-1$.

I. BETHE-HEITLER CROSS SECTION

Before proceeding to calculate the radiative corrections to the Bethe-Heitler cross section, it is necessary to discuss the properties of the Bethe-Heitler cross section itself. In particular we would like to discuss the treatment of form factors, the deep dip at symmetry, and a useful expansion of the cross section near symmetry. In Appendix A we discuss pair production from polarized photons. The result here may be of interest in the future to further test the Bethe-Heitler cross section. It is also important to know to what extent an accidentally polarized beam might change the cross section.

A. Cross Section and Definitions

Pair-production experiments have been performed by detecting the leptons completely, that is to say detecting both their angles and energies. If the mass of the nuclear final state is known, the kinematics is completely determined and the incoming photon energy can be calculated. The five variables detected are E_+ and E_-, the energies of the two leptons, θ_+ and θ_-, the angles made with the forward direction, and φ, the angle between the $(\mathbf{p}_+,\mathbf{k})$ plane and the $(\mathbf{p}_-,\mathbf{k})$ plane. Symbols used in treating pair production are defined in Table I. Exact symmetry is defined as $E_+=E_-$, $\theta_+=\theta_-$, and $\varphi=0$.

The Feynman diagrams for Bethe-Heitler pair production are shown in Fig. 1. The cross section in the laboratory is

$$d\sigma_{\mathrm{BH}}=\frac{\alpha^3Z^2}{16\pi^2}\frac{E_+E_-}{M_i}\frac{S(k)}{k\cdot P_f}M_{\mu\nu}N_{\mu\nu}dE_+d\Omega_+dE_-d\Omega_-, \quad (1.1)$$

[18] D. Yount and J. Pine, Phys. Rev. **128**, 1842 (1962).
[19] J. D. Bjorken and S. D. Drell, *Relativistic Quantum Mechanics* (McGraw-Hill Book Co., New York, 1964).

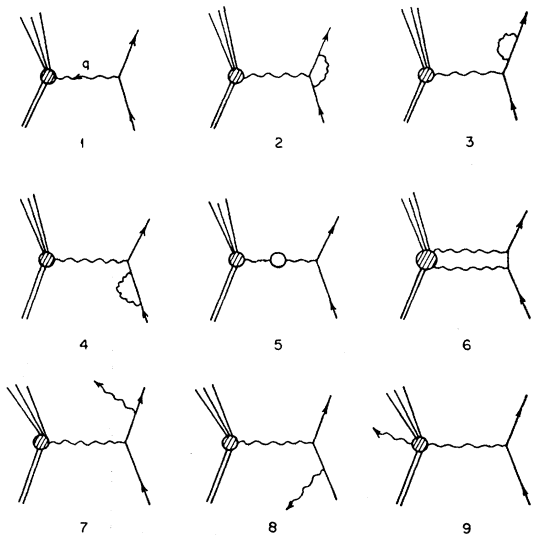

FIG. 5. Feynman diagrams for electron scattering and its radiative corrections.

where

$$M_{\mu\nu}=\frac{-2}{\beta_+\beta_-q^4}[(\beta_+^2+\beta_-^2+2q^2Q^2)g_{\mu\nu}+4q^2(p_{+\mu}p_{+\nu}+p_{-\mu}p_{-\nu})], \quad (1.2)$$

and

$$k=\frac{2k\cdot P_f}{2[M_i-E_+(1-\cos\theta_+)-E_-(1-\cos\theta_-)]},$$

$$2k\cdot P_f=M_f^2-M_i^2+2M_i(E_++E_-)-Q^2. \quad (1.3)$$

$S(k)$ is the incident photon spectrum. We have ignored m^2 terms.

B. Nuclear Form Factors

$N_{\mu\nu}$ in Eq. (1.1) can be written in general in terms of Drell-Walecka form factors[7]:

$$N_{\mu\nu}=4E_f\{W_1(q^2,q_0)[g_{\mu\nu}-q_\mu q_\nu/q^2]+W_2(q^2,q_0)(1/M_i^2)[P_{i\mu}-(P_i\cdot q/q^2)q_\mu]\times[P_{i\nu}-(P_i\cdot q/q^2)q_\nu]\}dq_0. \quad (1.4)$$

These form factors can be determined from electron-nucleus scattering as discussed in the Introduction, but at present such a program is difficult to carry out experimentally. Therefore, it is convenient to take advantage of the low momentum transfers involved in elastic symmetric pair production to approximate $N_{\mu\nu}$. For $|q^2/M_i^2|\ll 1$ and a nucleus of any spin, we may write for the elastic and quasi-elastic part of $N_{\mu\nu}$,

$$N_{\mu\nu}\cong G_E^2(q^2)R_\mu R_\nu, \quad (1.5)$$

where $M_f^2=M_i^2$, and k is defined by $2k\cdot P_f=2M_i(E_++E_-)-Q^2$. [See Eq. (1.3).] The inelastic part of $N_{\mu\nu}$ does not become significant until it is kinematically possible to excite a nuclear resonance

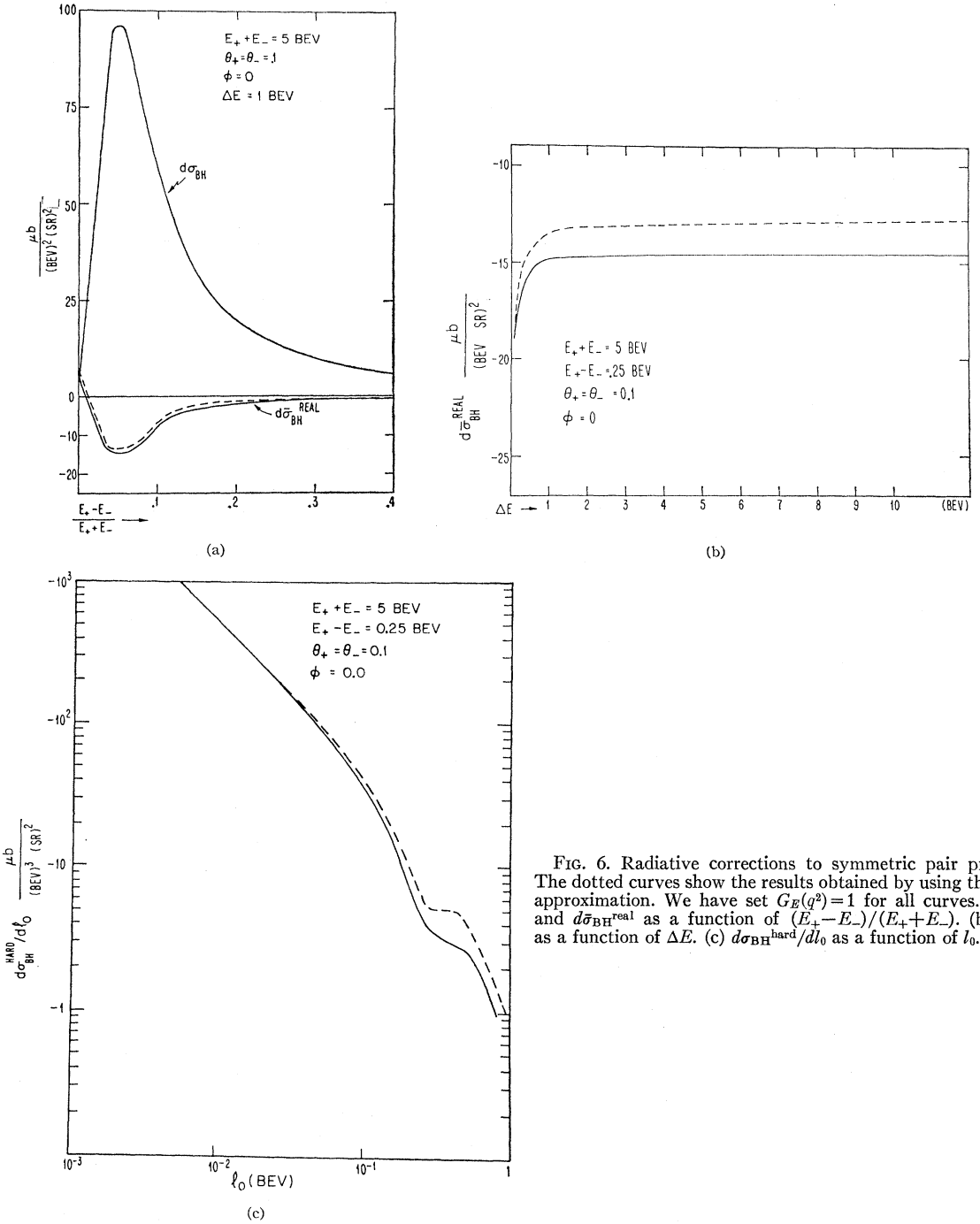

FIG. 6. Radiative corrections to symmetric pair production. The dotted curves show the results obtained by using the peaking approximation. We have set $G_E(q^2)=1$ for all curves. (a) $d\sigma_{\rm BH}$ and $d\tilde{\sigma}_{\rm BH}{}^{\rm real}$ as a function of $(E_+-E_-)/(E_++E_-)$. (b) $d\tilde{\sigma}_{\rm BH}{}^{\rm real}$ as a function of ΔE. (c) $d\sigma_{\rm BH}{}^{\rm hard}/dl_0$ as a function of l_0.

and then the $1/q^4$ factor in the cross section has effectively cut off the contribution.

C. Dip and Expansion Around Symmetry

At symmetry $\beta_+=\beta_-=-k\cdot q$ and $2p_+\cdot R=2p_-\cdot R=k\cdot R$. In addition $(k\cdot q)^2R^2+q^2(k\cdot R)^2=0$. This latter fact may be seen most easily by transforming to the Lorentz frame in which the initial and final nuclear states have the same energy. Near symmetry the cross section is rapidly increasing due to the factor $1/q^4$, but it is cut off at symmetry by $(k\cdot q)^2R^2+q^2(k\cdot R)^2=0$, leaving, if we use Eq. (1.5) for $N_{\mu\nu}$,

$$[M_{\mu\nu}R_\mu R_\nu]_{\rm sym}=(-2/\beta_+\beta_-q^4)(2q^2Q^2R^2), \quad (1.6)$$

where $q^2Q^2R^2/q^2(k\cdot R)^2\sim\theta^2$. Therefore there is a dip in the cross section at symmetry which becomes deeper

and narrower as θ decreases. [See Fig. 6(a) for a graph of the cross section near symmetry.]

The existence of the dip has two consequences as far as radiative corrections are concerned. First, since the function $1/q^4$ is cut off at symmetry in the Bethe-Heitler cross section, one may argue that if some terms in the virtual radiative correction are not similarly cut off, the correction may become very large at symmetry even though it is small everywhere else. It can be shown, however, that all virtual radiative corrections to the Bethe-Heitler cross section involving a one-photon exchange with the nucleus have a dip, thereby settling any uneasiness on this point.[17] Virtual corrections involving two or more photons exchanged with the nucleus pose no problem since they do not contain the photon propagator squared, $1/q^4$. Secondly, the dip is so narrow that it has not been resolved experimentally. The pairs detected in an experiment come primarily from the peak a little off symmetry. For this reason the value of the cross section at symmetry has very little to do with the cross section determined from experiment. Similarly one may suspect that a calculation of the radiative corrections limited to the exactly symmetric situation is unreliable.

In dealing with the Bethe-Heitler cross section and its radiative corrections, it is often convenient to expand around symmetry. In this we follow Ref. 1 and expand in the variables $a=(\theta_+-\theta_-)/(\theta_++\theta_-)$, $\epsilon=(E_+-E_-)/(E_++E_-)$, $\theta=\frac{1}{2}(\theta_++\theta_-)$, $E=\frac{1}{2}(E_++E_-)$, and φ. This approximation includes the approximation of no recoil for the nucleus. We use Eq. (1.5) for $N_{\mu\nu}$.

The cross section becomes

$$d\sigma_{\rm BH}=d\sigma_{\rm BH}({\rm sym})\frac{[(a+\epsilon)^2+\frac{1}{4}\varphi^2+\frac{1}{4}\theta^4]}{4[(a+\epsilon)^2+\frac{1}{4}\theta^2+\frac{1}{4}\varphi^2]},$$

$$d\sigma_{\rm BH}({\rm sym})=\frac{\alpha^3Z^2}{2\pi^2}\frac{1}{\theta^6E^3}S(2E)G_E{}^2(q^2)\times dE_+d\Omega_+dE_-d\Omega_-. \quad (1.7)$$

If a, ϵ, φ, and θ are all less than $1/10$, then the above expansion is good to better than 1%, not including the error introduced by ignoring inelastic form factors. In Eq. (1.7) the $\frac{1}{4}\theta^4$ term should strictly speaking be ignored, but it has been included to show the behavior of the cross section at exact symmetry.

II. VIRTUAL PHOTON CORRECTION

The Feynman diagrams involved in the virtual photon correction to pair production are shown in Fig. 2. The radiative correction to order α^4 is due to the interference of these diagrams with the Bethe-Heitler diagrams of Fig. 1. As pointed out in the Introduction, however, to this order in α, diagrams Fig. 2–15 to Fig. 2–18 do not contribute to symmetric pair production since their interference with the Bethe-Heitler diagrams is antisymmetric in $p_+\leftrightarrow p_-$. In the remaining diagrams (Figs. 2–1 to 2–14) the virtual photon exchanges involve only the leptonic part leaving the nuclear current unaffected. Thus the form factors entering the virtual photon radiative correction are the same as the ones entering the basic Bethe-Heitler process.

In calculating the radiative corrections, only one assumption will be made, namely, that m^2 is small compared to other invariants or

$$m^2/Q^2\ll 1;\quad m^2/\beta_\pm\ll 1;\quad m^2/-q^2\ll 1. \quad (2.1)$$

The cross section for the virtual photon radiative correction is [see Eq. (1.1)]

$$d\sigma_{\rm BH}{}^{\rm vir}=\frac{\alpha^3Z^2}{16\pi^2}\frac{E_+E_-}{M_i}\frac{S(k)}{k\cdot P_f}M_{\mu\nu}{}^{\rm vir}N_{\mu\nu}\times dE_+d\Omega_+dE_-d\Omega_-. \quad (2.2)$$

$M_{\mu\nu}{}^{\rm vir}$ is given for the general case in Appendix B. In calculating it we used the procedure of Brown and Feynman.[20] The divergences were handled in the usual way by letting the photon have a small mass λ and, in addition, imposing a high-energy cutoff on the photon propagator. After renormalization the result does not depend on the high-energy cutoff. The general result, Eq. (B1), is useful for finding the virtual photon correction not only to pair production but also to bremsstrahlung and trident production as discussed in the Appendix.

$M_{\mu\nu}{}^{\rm vir}$ is not in a form which can be applied easily to an experimental situation, but there is no way to simplify it without making further assumptions. These assumptions must naturally be guided by the particular experimental situation at issue. Here we specialize to pair production near symmetry, where $|q^2/Q^2|\ll 1$. The result is

$$d\sigma_{\rm BH}{}^{\rm vir}=(\alpha/2\pi)\{-2H_0(Q^2)-2\ln(\lambda^2/m^2)+\tfrac{3}{2}\ln(\beta_+/m^2)+\tfrac{3}{2}\ln(\beta_-/m^2)+\tfrac{4}{3}\ln(-q^2/m^2)-65/9+(\ln 2)^2+[4(\ln 2)^2-2\ln 2+2]\}d\sigma_{\rm BH}. \quad (2.3)$$

Here we have set $\ln(Q^2/\beta_\pm)\cong\ln 2$. The small term in parentheses comes from all but the first term of Eq. (B1), which is to say from terms where the Bethe-Heitler matrix element cannot, in general, be factored out. However, near symmetry, where the dip enforces a certain uniformity on all terms, factorization is possible. We discover this by help of the expansion discussed in Sec. I C. $H_0(Q^2)+\ln(\lambda^2/m^2)$ contains the infrared divergence and will cancel against a similar term in the soft-photon correction.

III. REAL PHOTON CORRECTION

A. Introduction and General Formulation

The Feynman diagrams involved in the real photon correction are shown in Fig. 3. The radiated photon is

[20] L. M. Brown and R. P. Feynman, Phys. Rev. 85, 231 (1952).

undetected. To find the radiative correction, we must square the matrix element corresponding to the diagrams of Fig. 3, sum over spins and polarizations, and integrate over the final states of the radiated photon. As pointed out in the Introduction, diagrams Fig. 3–7 and Fig. 3–8 do not contribute to symmetric pair production. In the remaining diagrams the photon is radiated only from the leptonic part leaving the nuclear current unaffected. Thus the form factors entering the real photon corrections to symmetric pair production are the same as the ones entering the basic Bethe-Heitler process.

The cross section for the real photon correction is

$$d\sigma_{\mathrm{BH}}{}^{\mathrm{real}}=\frac{\alpha^3Z^2}{16\pi^2}\frac{E_+E_-}{M_i}\frac{\alpha}{\pi}\int\frac{d^3l}{4\pi l_0}\frac{S(k)}{k\cdot P_f}M_{\mu\nu}{}^{\mathrm{real}}N_{\mu\nu}\times dE_+d\Omega_+dE_-d\Omega_-, \quad (3.1)$$

where

$$2k\cdot P_f=M_f{}^2-(P_i-p_+-p_--l)^2,$$
$$2l\cdot P_f=M_i{}^2-M_f{}^2+2M_i(k-E_+-E_-)+q^2,$$
$$l_0=2l\cdot P_f/2[M_i+k(1-\cos\theta_{lk})-E_+(1-\cos\theta_{lp_+})-E_-(1-\cos\theta_{lp_-})], \quad (3.2)$$

and

$$\cos\theta_{lp}=\mathbf{l}\cdot\mathbf{p}/|\mathbf{l}||\mathbf{p}|;\quad p=p_+,p_-,k. \quad (3.3)$$

In general, one would perform the integral first over the angles of $\mathbf{l}$ and then over the possible values of k up to $k_{\max}$. l_0 depends on the direction of $\mathbf{l}$ as shown in Eq. (3.2) and this complicated dependence makes the exact performance of the integral extremely difficult except by numerical methods.

For low q^2, the dependence of l_0 on the direction of $\mathbf{l}$ is slight. For such cases

$$l_0M_f\cong l\cdot P_f. \quad (3.4)$$

This is a particularly good approximation for the small recoil situation of symmetric pair production off carbon.

B. Soft-Photon Correction

In order to extract the infrared divergent terms from the real photon correction, we split the integration in Eq. (3.1) into two parts, the soft-photon part with $0\leq l_0\leq\delta$ and the hard-photon part with the possible values of $l_0\geq\delta$, where $\delta<<<m$. In the soft-photon part we ignore all terms in $M_{\mu\nu}{}^{\mathrm{real}}$ except the ones of order l_0^{-2} and we ignore as well the kinematical dependence on l. No approximation is involved here since at the end of the complete calculation we will let $\delta\to 0$. Then we can write, letting the photon have a small mass λ,[8]

$$d\sigma_{\mathrm{BH}}{}^{\mathrm{soft}}=\frac{\alpha}{\pi}\int_0^\delta dl\int\frac{|\mathbf{l}|^2d\Omega}{(|\mathbf{l}|^2+\lambda^2)^{1/2}}\times\frac{1}{4\pi}\left(\frac{8p_+\cdot p_-}{l_+l_-}-\frac{4m^2}{l_+{}^2}-\frac{4m^2}{l_-{}^2}\right)d\sigma_{\mathrm{BH}} \quad (3.5)$$

or

$$d\sigma_{\mathrm{BH}}{}^{\mathrm{soft}}=\frac{\alpha}{\pi}\left[\left(\ln\frac{Q^2}{m^2}-1\right)\ln\frac{\delta^2}{E_+E_-}-\tfrac{1}{2}Y(p_+,p_-)-L\left(\frac{E_+-E_-}{E_-}\right)-L\left(\frac{E_--E_+}{E_+}\right)-\tfrac{1}{6}\pi^2+H_0(-Q^2)+\ln\frac{\lambda^2}{m^2}\right]d\sigma_{\mathrm{BH}}, \quad (3.6)$$

where

$$Y(p_+,p_-)=Q^2\int_0^1\frac{dx}{p_x{}^2}\left[\frac{E_x-|\mathbf{p}_x|}{|\mathbf{p}_x|}\ln\frac{E_x+|\mathbf{p}_x|}{E_x-|\mathbf{p}_x|}+2\ln\frac{E_x+|\mathbf{p}_x|}{2E_x}\right],$$
$$p_x=p_+x+p_-(1-x).$$

$H_0(Q)$ is given in Appendix B as an integral. By performing the integral, it can be shown that $H_0(-Q^2)=H_0(Q^2)-\frac{1}{2}\pi^2$ for $m^2/Q^2\ll 1$. The difference of $\frac{1}{2}\pi^2$ arises because $H_0(Q^2)$ has a pole in the integrand while $H_0(-Q^2)$ does not. Notice that Eq. (3.5) is invariant under $p_\pm\to -p_\pm$ and therefore independent of whether the charged particles are incoming or outgoing. This is not true for the virtual correction. Thus for pair production the sum of the infrared terms $H_0+\ln(\lambda^2/m^2)$ in the virtual- and soft-photon correction produces a π^2 term, while for bremsstrahlung the cancellation is complete. $L(x)$ is the Spence function and is defined in Appendix B.[21] For pair production near symmetry, $Y(p_+,p_-)\sim\theta^2$ and

$$L\left(\frac{E_+-E_-}{E_-}\right)+L\left(\frac{E_--E_+}{E_+}\right)+\tfrac{1}{6}\pi^2\cong\frac{(E_+-E_-)^2}{E^2}.$$

These terms can therefore be ignored.

C. Hard-Photon Correction

To calculate the hard-photon correction we must find $M_{\mu\nu}{}^{\mathrm{real}}$. Though the procedure is involved and intermediate expressions are long, the final result combines into a relatively simple form.

A computer was used to calculate the traces. The program was written and executed by Parsons in connection with another problem.[22] The output, some 500 terms, was then manipulated by hand in search of a useful expression.[23] The result is

$$d\sigma_{\mathrm{BH}}{}^{\mathrm{hard}}=\frac{\alpha^3Z^2}{16\pi^2}\frac{E_+E_-}{M_i}\frac{\alpha}{\pi}\int_\delta^{l_0(\max)}dl_0\int\frac{l_0d\Omega}{4\pi}\frac{S(k)}{k\cdot P_f}\times M_{\mu\nu}{}^{\mathrm{real}}N_{\mu\nu}dE_+d\Omega_+dE_-d\Omega_-, \quad (3.7)$$

[21] K. Mitchell, Phil. Mag. **40**, 351 (1949).
[22] R. G. Parsons, Phys. Rev. **150**, 1165 (1966).
[23] Such a complicated effort is not necessary. Equation (3.8) can be proven in general and quite simply by using the Ward identity. This will be discussed in a subsequent paper by the author.

where

$$M_{\mu\nu}{}^{\text{real}}N_{\mu\nu}=\left[\frac{8p_+\cdot p_-}{l_+l_-}\left(1+\frac{1}{2}\frac{l_+^2+l_-^2}{Q^2(Q^2+l_+\cdot l_-)}\right)-\frac{4m^2}{l_+^2}-\frac{4m^2}{l_-^2}\right]\frac{1}{q_l^4}M_{\text{BH}}(p_+',p_-')+F(l)\frac{8p_+\cdot p_-}{l_+l_-q_l^4},\quad(3.8)$$

with

$$p_+'+p_-'=p_++p_-+l,$$

$$p_+'-p_-'=p_+\left(1+\frac{l\cdot p_-}{p_+\cdot p_-}\right)-p_-\left(1+\frac{l\cdot p_+}{p_+\cdot p_-}\right),$$

$$q_l^2=(k-p_+-p_--l)^2,$$

and $M_{\text{BH}}(p_+,p_-)=q^4M_{\mu\nu}N_{\mu\nu}$. [See Eqs. (1.2) and (1.3).]

The function $F(l)$ is complicated. We have not been able to calculate it here, but instead have found that it satisfies two conditions which in most cases are sufficient to make the $F(l)$ term negligible.

(1) $F(l)$ is of order l_0^2 and above. This means that the $F(l)$ term in Eq. (3.8) is of order 1 in l_0, two order of l_0 removed from the first term of order l_0^{-2}. Most experiments are performed such that $l_0(\max)/E_\pm\ll1$, where $l_0(\max)$ is the maximum allowed value of l_0, thus assuring that the $F(l)$ term is small. For symmetric pair production the relevant ratio $l_0/E_\pm$ is determined not by the value of $l_0(\max)$ but by the shape of the strongly peaked Bethe-Heitler cross section. The important ratio for this case is $l_0/E_\pm\sim\theta$. Thus for pair production at 5° the consequence of ignoring $F(l)$ introduces at most only a 1% error in the correction. The second condition on $F(l)$ further reduces this error.

(2) $F(\mathbf{l}\|\mathbf{p}_+)=0$ and $F(\mathbf{l}\|\mathbf{p}_-)=0$. This condition is closely related to the peaking approximation discussed in the next subsection. The factor $p_+\cdot p_-/l_+l_-$ is strongly peaked when $\mathbf{l}\|\mathbf{p}_+$ or $\mathbf{l}\|\mathbf{p}_-$, corresponding to the fact that photons are radiated mostly in the direction of motion of highly relativistic charged particles. Thus, while the first term of Eq. (3.8) becomes very large at $\mathbf{l}\|\mathbf{p}_+$ or $\mathbf{l}\|\mathbf{p}_-$, the $F(l)$ term remains always small. The result of the condition is to reduce the $F(l)$ term further with respect to the first term of Eq. (3.8).

The above conditions on $F(l)$ were determined by combining terms to order l_0^{-1} and finding that to this order the result fitted into Eq. (3.8) without the $F(l)$ term. Then, for the remainder of the calculation, we assumed $\mathbf{l}\|\mathbf{p}_+$ and showed to all orders in l_0 that the nonzero terms combined into Eq. (3.8) without the $F(l)$ term and where now $\mathbf{l}\|\mathbf{p}_+$. The calculation was repeated for $\mathbf{l}\|\mathbf{p}_-$ as a check.

$d\sigma_{\text{BH}}{}^{\text{hard}}$ may be integrated numerically, using the kinematical relations given in Eq. (3.2). The error made in ignoring $F(l)$ would be less than 1% *of the correction* for symmetric pair production. This is indeed completely negligible.

D. Peaking Approximation

The peaking approximation is commonly used to reduce the difficulty of calculating the hard-photon correction.[24–27] It relies on the fact that the emitted photon is given off dominantly in the direction of motion of the highly relativistic radiating particle. This corresponds to the strong peaking of $p_+\cdot p_-/l_+l_-$ when $\mathbf{l}\|\mathbf{p}_+$ or $\mathbf{l}\|\mathbf{p}_-$. Near these points

$$l_\pm=2p_\pm\cdot l\to E_\pm l_0\left[\theta_{lp_\pm}{}^2+\frac{m^2}{E_\pm{}^2}\right].\quad(3.9)$$

Taking advantage of the peaking, one may approximate angular integrals as follows:

$$\int\frac{l_0^2d\Omega}{4\pi}\frac{8p_+\cdot p_-}{l_+l_-}f(l)\cong\tfrac{1}{2}[f(\mathbf{l}\|\mathbf{p}_+)+f(\mathbf{l}\|\mathbf{p}_-)]\times\int\frac{l_0^2d\Omega}{4\pi}\frac{8p_+\cdot p_-}{l_+l_-}=[f(\mathbf{l}\|\mathbf{p}_+)+f(\mathbf{l}\|\mathbf{p}_-)]\ln\frac{Q^2}{m^2},$$

$$\int\frac{l_0^2d\Omega}{4\pi}\frac{4m^2}{(l_\pm)^2}f(l)\cong f(\mathbf{l}\|\mathbf{p}_\pm)\int\frac{l_0^2d\Omega}{4\pi}\frac{4m^2}{(l_\pm)^2}=f(\mathbf{l}\|\mathbf{p}_\pm),\quad(3.10)$$

where $f(l)$ is any function which varies reasonably slowly over the region of integration. The condition $Q^2/m^2\gg1$ must hold. The factor $\ln(Q^2/m^2)-1$ is not unique due to the fact that when the two peaks in $p_+\cdot p_-/l_+l_-$ overlap for small θ the proper limits of integration in the approximation are uncertain. We choose the above form so that the hard-photon cross section reduces to the correct limit as $l_0\to0$ (soft-photon limit). Unless this is done, the soft- and hard-photon parts of the radiative correction do not combine properly into a divergence-free result as $\delta\to0$.

Applying the peaking approximation to Eqs. (3.7) and (3.8) we get

$$d\sigma_{\text{BH}}{}^{\text{hard}}\cong\frac{\alpha}{\pi}\int_\delta^{l_0(\max+)}\frac{dl_0}{l_0}d\sigma_{\text{BH}}(E_++l_0,E_-)\frac{E_+}{E_++l_0}\times\left[\left(1+\frac{1}{2}\frac{l_0^2}{E_+(E_++l_0)}\right)\ln\frac{Q^2}{m^2}-1\right]+\frac{\alpha}{\pi}\int_\delta^{l_0(\max-)}\frac{dl_0}{l_0}d\sigma_{\text{BH}}(E_+,E_-+l_0)\frac{E_-}{E_-+l_0}\times\left[\left(1+\frac{1}{2}\frac{l_0^2}{E_-(E_-+l_0)}\right)\ln\frac{Q^1}{m^2}-1\right].\quad(3.11)$$

[24] Y. S. Tsai, Phys. Rev. **120**, 269 (1960).
[25] A. S. Krass, Phys. Rev. **125**, 2172 (1962).
[26] N. T. Meister and T. A. Griffy, Phys. Rev. **133**, B1032 (1964).
[27] R. Atkinson III, thesis, Stanford University, 1965 (unpublished).

The designations $l_0(\max\pm)$ indicate that $l_0(\max)$ depends on the angle of $\mathbf{l}$, which has been taken to be predominantly parallel to $\mathbf{p}_+$ and $\mathbf{p}_-$.

The peaking approximation is extremely useful because it allows us to write a formula like Eq. (3.11) for any scattering problem. We will discuss this fact in detail in a subsequent paper.

The remaining integral in Eq. (3.11) can be performed analytically, provided we use the expansion of the Bethe-Heitler cross section near symmetry given in Eq. (1.7). The result is given in Appendix C. The main error in this result lies in making the peaking approximation and it goes like $\ln(1/\theta^2)/\ln(Q^2/m^2)$.

IV. DISCUSSION

The total radiative correction to order α^4 can now be written as follows for symmetric pair production:

$$d\sigma_{\mathrm{BH}}+d\sigma_{\mathrm{BH}}{}^{\mathrm{rad}}$$
$$=d\sigma_{\mathrm{BH}}+d\sigma_{\mathrm{BH}}{}^{\mathrm{vir}}+\lim_{\delta\to 0}[d\sigma_{\mathrm{BH}}{}^{\mathrm{soft}}+d\sigma_{\mathrm{BH}}{}^{\mathrm{hard}}]$$
$$=\left\{1+\frac{\alpha}{2\pi}\left[\tfrac{3}{2}\ln\frac{\beta_+}{m^2}+\tfrac{3}{2}\ln\frac{\beta_-}{m^2}+\tfrac{4}{3}\ln\frac{-q^2}{m^2}-65/9\right.\right.$$
$$\left.\left.+5(\ln 2)^2-2\ln 2+2-\pi^2\right]\right\}d\sigma_{\mathrm{BH}}+d\bar{\sigma}_{\mathrm{BH}}{}^{\mathrm{real}}, \quad (4.1)$$

where

$$d\bar{\sigma}_{\mathrm{BH}}{}^{\mathrm{real}}=\lim_{\delta\to 0}\left[-\frac{\alpha}{\pi}\left(\ln\frac{Q^2}{m^2}-1\right)\right.$$
$$\left.\times\ln\frac{E_+E_-}{\delta^2}+d\sigma_{\mathrm{BH}}{}^{\mathrm{hard}}\right]. \quad (4.2)$$

$d\sigma_{\mathrm{BH}}{}^{\mathrm{hard}}$ is given by Eqs. (3.7) and (3.8), ignoring the $F(l)$ term. The error in the result is negligible ($\sim 1\%$ of the correction). The correction to higher orders in α may be estimated by exponentiation. For practical purposes it is sufficient to set $\delta/E\ll\frac{1}{2}\theta$ for use in a numerical integration of $d\sigma_{\mathrm{BH}}{}^{\mathrm{hard}}$.

In Fig. 6 we have plotted $d\bar{\sigma}_{\mathrm{BH}}{}^{\mathrm{real}}$ and $d\sigma_{\mathrm{BH}}{}^{\mathrm{hard}}/dl_0$ for some typical configurations. For comparison we have also plotted the results using the approximate expressions Eq. (C1) for $d\sigma_{\mathrm{BH}}{}^{\mathrm{hard}}$ and Eq. (3.11) for $d\sigma_{\mathrm{BH}}{}^{\mathrm{hard}}/dl_0$. Note in particular in Fig. 6(b) that the real photon correction at the peak of the Bethe-Heitler cross section is virtually independent of ΔE. The reason is that the radiation of a high-energy photon forces the modified cross section [see Eq. (3.11)] far away from the peak and therefore the event does not contribute significantly. This differs from the result of Lomon[12] based on an inadequate approximation of the Bethe-Heitler cross section.

In comparing our result with the result of Bjorken, Drell, and Frautschi [Eq. (1)], we must compare $d\sigma_{\mathrm{BH}}{}^{\mathrm{rad}}-d\bar{\sigma}_{\mathrm{BH}}{}^{\mathrm{real}}$ with the first term of Eq. (1) and $d\bar{\sigma}_{\mathrm{BH}}{}^{\mathrm{real}}$ with the second term. $|d\bar{\sigma}_{\mathrm{BH}}{}^{\mathrm{real}}|$ is about three times larger than the comparable term in Eq. (1). The difference in these results is due, of course, to the different treatment of $d\sigma_{\mathrm{BH}}{}^{\mathrm{hard}}$. [See Eq. (4.2).] The rapid variation of the Bethe-Heitler cross section near symmetry makes it imperative that such variation be considered when calculating $d\sigma_{\mathrm{BH}}{}^{\mathrm{hard}}$. This was not done by Bjorken, Drell, and Frautschi who used the soft-photon approximation in calculating their real photon correction. $d\sigma_{\mathrm{BH}}{}^{\mathrm{rad}}-d\bar{\sigma}_{\mathrm{BH}}{}^{\mathrm{real}}$ also differs from the comparable result of Eq. (1). Notice in particular that the constant term $65/9+\pi^2$ contributes significantly to the correction. As we have seen in Sec. III B, the π^2 term arises rather simply from a consideration of the infrared-divergent terms. The 65/9 term, however, as well as other constant terms of Eq. (4.1), can only be obtained from a detailed calculation of the diagrams of Fig. 2. $d\sigma_{\mathrm{BH}}{}^{\mathrm{rad}}-d\bar{\sigma}_{\mathrm{BH}}{}^{\mathrm{real}}$ is about $+4\%$ of the Bethe-Heitler cross section for $E_+=E_-=5$ BeV, $\theta_+=\theta_-=0.1$, and is fairly constant for all points near symmetry. [Compare with $d\bar{\sigma}_{\mathrm{BH}}{}^{\mathrm{real}}$ given for the same points in Figs. 6(a) and 6(b).]

The peaking approximation is seen to duplicate the behavior of the exact result rather well. The deviation is about 10% at the peak and somewhat larger away from the peak.

ACKNOWLEDGMENTS

I would like to express my deep gratitude to Professor Frank M. Pipkin for his continual encouragement and support. Also, I would like to thank Professor E. L. Lomon, Dr. Robert Perrin, Dr. George R. Henry, K. Randolph, and J. Tenenbaum for useful conversations. I am grateful to Dr. R. G. Parsons for permission to use the results of his computer calculation of traces.

APPENDIX A: PAIR PRODUCTION FROM POLARIZED PHOTONS

In calculating the Bethe-Heitler cross section in Sec. I, we assumed that the incident photon beam was unpolarized. In this Appendix we drop that assumption and calculate the cross section if the photons are polarized with polarization vector e_μ. It is important to know if one polarization contributes dominantly in any given experimental situation. If such is the case, an accidentally polarized beam might affect the result expected.

The Bethe-Heitler cross section for photons of polarization e_μ is

$$d\sigma_{\mathrm{BH}}{}^{e}=\frac{\alpha^3Z^2}{16\pi^2}\frac{E_+E_-}{M_i}\frac{S(k)}{k\cdot P_f}M_{\mu\nu}{}^{e}N_{\mu\nu}dE_+d\Omega_+dE_-d\Omega_-,$$
$$M_{\mu\nu}{}^{e}=\frac{-4}{\beta_+\beta_-q^4}\{2q^2k_\mu k_\nu+\tfrac{1}{2}(\beta_++\beta_-)^2g_{\mu\nu}+\tfrac{1}{2}\beta_+\beta_-q^2(\ )_-{}^2g_{\mu\nu}$$
$$+[(\ )_+k_\mu+(\ )_-\Delta_\mu][(\ )_+k_\nu+(\ )_-\Delta_\nu]\tfrac{1}{2}\beta_+\beta_-$$
$$+2\beta_+\beta_-e_\mu e_\nu-2\beta_+\beta_-e_\nu[(\ )_+k_\mu+(\ )_-\Delta_\mu]\}, \quad (A1)$$

where

$$(\ )_{\pm}=\left(\frac{2p_+\cdot e}{\beta_+}\pm\frac{2p_-\cdot e}{\beta_-}\right),$$

and the remaining symbols are defined in Table I. At symmetry $e\cdot R=(\ )_+=0$ and the result reduces to

$$M_{\mu\nu}{}^{e}R_\mu R_\nu=-(2/q^2)(\ )_-{}^2R^2. \tag{A2}$$

If we choose the two states of polarization to be perpendicular and parallel to the $\mathbf{p}_+,\mathbf{p}_-$ plane, then only the parallel polarization contributes at symmetry. Because of the dip, however, it is not experimentally relevant what the result is at symmetry but rather what the result is slightly off symmetry. To determine this we use the expansion method described in Sec. I C. Let us define the polarization vector with respect to a plane containing $\mathbf{k}$ and making an angle $\frac{1}{2}\varphi$ with the $(\mathbf{p}_+,\mathbf{k})$ plane and so also with the $(\mathbf{p}_-,\mathbf{k})$ plane. Now

$$\begin{aligned}p_+\cdot e_\perp&=-E_+\sin\theta_+\sin\tfrac{1}{2}\varphi,\\ p_-\cdot e_\perp&=-E_-\sin\theta_-\sin\tfrac{1}{2}\varphi,\end{aligned} \tag{A3}$$

where $e_\perp$ ($e_{\parallel}$) is the polarization vector perpendicular (parallel) to the defined plane. Expanding around symmetry

$$\begin{aligned}d\sigma_{\rm BH}{}^{e_\perp}&=d\sigma_{\rm BH}(\rm sym)\\ &\quad\times(a+\epsilon)^2/2[(a+\epsilon)^2+\tfrac{1}{4}\theta^2+\tfrac{1}{4}\varphi^2],\\ d\sigma_{\rm BH}{}^{e_{\parallel}}&=d\sigma_{\rm BH}(\rm sym)\\ &\quad\times(\tfrac{1}{4}\varphi^2+\tfrac{1}{4}\theta^4)/2[(a+\epsilon)^2+\tfrac{1}{4}\theta^2+\tfrac{1}{4}\varphi^2].\end{aligned} \tag{A4}$$

Clearly, if we average over the two polarizations, we retrieve the result Eq. (1.7).

A consequence of the above result is that pair production near symmetry can be used as an analyzer of polarization. The term $\frac{1}{4}\theta^4$ can be ignored. Then, if the experimental acceptance is taken to be a slit with $\varphi\ll\theta$, only photons polarized perpendicular to the slit will contribute to pair production.

APPENDIX B: GENERAL VIRTUAL PHOTON CORRECTION

Here we give the general result for the virtual photon correction to pair production (see Sec. II). Symbols are defined in Table I.

$$\begin{aligned}M_{\mu\nu}{}^{\rm vir}=&(\alpha/4\pi)[F_1{}^+{+}F_1{}^-]M_{\mu\nu}+(\alpha/2\pi)(4/\beta_+\beta_-q^4)\{F_1{}^+[(p_{+\mu}{+}p_{-\mu})(p_{-\nu}\beta_-{-}p_{+\nu}\beta_+){+}\tfrac{1}{4}(\beta_+{}^2{-}\beta_-{}^2)g_{\mu\nu}]\\ &+(F_2{}^+{-}F_3{}^-)[-p_{+\mu}\beta_+(p_{-\nu}\beta_-{-}p_{+\nu}\beta_+){-}q^2p_{+\mu}\beta_+(p_{-\nu}{-}p_{+\nu}){+}\tfrac{1}{2}Q^2\beta_+(\beta_-{+}q^2)g_{\mu\nu}]\\ &+(F_4{}^+{-}F_5{}^-)[p_{+\mu}Q^2(p_{-\nu}\beta_-{-}p_{+\nu}\beta_+){+}p_{+\mu}q^2(p_{+\nu}\beta_-{-}p_{-\nu}\beta_+)]\\ &+F_6{}^+[(p_{-\mu}p_{-\nu}\beta_-{}^2{-}p_{+\mu}p_{+\nu}\beta_+{}^2){+}q^2(p_{+\mu}{+}p_{-\mu})(p_{-\nu}\beta_-{-}p_{+\nu}\beta_+){+}\tfrac{1}{2}(\beta_-{-}\beta_+)\beta_+\beta_-g_{\mu\nu}]\\ &+(F_7{}^+{-}F_9{}^-)[p_{+\mu}\beta_+\beta_-(p_{-\nu}\beta_-{-}p_{+\nu}\beta_+){-}p_{+\mu}p_{+\nu}q^2(2\beta_+\beta_-{+}q^2\beta_-){-}p_{+\mu}p_{-\nu}q^2Q^2\beta_-]\\ &+(F_8{}^+{-}F_{10}{}^-)[p_{+\mu}\beta_+\beta_-(p_{-\nu}\beta_-{-}p_{+\nu}\beta_+){+}p_{+\mu}p_{+\nu}q^2Q^2\beta_+{+}p_{+\mu}p_{-\nu}q^2(2\beta_+\beta_-{+}q^2\beta_+)]{+}\text{same with } p_+\leftrightarrow p_-\}.\end{aligned} \tag{B1}$$

In writing this result we have used the fact that $q_\mu N_{\mu\nu}=0$ and $N_{\mu\nu}=N_{\nu\mu}$. The functions $F_n{}^\pm$ are given below.

$$F_1{}^+=\left[-2H_0(Q^2)-2\ln\frac{\lambda^2}{m^2}+2J_{00}{}^+{+}3\ln\left|\frac{\beta_+}{m^2}\right|+\tfrac{4}{3}\ln\left|\frac{q^2}{m^2}\right|-\frac{65}{9}-\frac{3q^2}{\beta_+{+}q^2}\ln\left|\frac{\beta_+}{q^2}\right|\right],$$

$$F_2{}^+=\left[-\frac{2}{Q^2}\ln\left|\frac{Q^2}{\beta_+}\right|-\frac{2q^2}{Q^2(\beta_+{+}\beta_-)}\ln\left|\frac{Q^2}{q^2}\right|-\frac{1}{\beta_+}-\frac{1}{\beta_-}J_{00}{}^+\right],$$

$$F_3{}^+=\left[-\frac{\beta_+Q^2{+}2\beta_+\beta_-}{\beta_-Q^2(\beta_+{+}q^2)}\ln\left|\frac{Q^2}{\beta_+}\right|-\frac{q^2(\beta_+Q^2{+}3\beta_-Q^2{+}2\beta_+\beta_-)}{\beta_-Q^2(\beta_+{+}\beta_-)(\beta_+{+}q^2)}\ln\left|\frac{Q^2}{q^2}\right|+\frac{\beta_+{+}2\beta_-}{\beta_-{}^2}J_{00}{}^+\right],$$

$$F_4{}^+=\left[\frac{2\beta_-{+}Q^2}{Q^2\beta_-}\ln\left|\frac{Q^2}{\beta_+}\right|+\frac{q^2(2\beta_-{+}Q^2)}{Q^2\beta_-(\beta_+{+}\beta_-)}\ln\left|\frac{Q^2}{q^2}\right|-\frac{\beta_+{+}2\beta_-{+}q^2}{\beta_-{}^2}J_{00}{}^+\right],$$

$$\begin{aligned}F_5{}^+=\Bigg[&\frac{2\beta_+\beta_-(\beta_+{+}q^2){+}q^2Q^2(\beta_+{-}\beta_-{+}q^2)}{Q^2\beta_-(\beta_+{+}q^2)^2}\ln\left|\frac{Q^2}{\beta_+}\right|+\frac{1}{\beta_+{+}q^2}\\ &+\frac{q^2(Q^2\beta_-{}^2{+}2\beta_+\beta_-(Q^2{+}\beta_+{+}q^2){+}Q^4q^2)}{Q^2\beta_-(\beta_+{+}\beta_-)(\beta_+{+}q^2)^2}\ln\left|\frac{Q^2}{q^2}\right|+\frac{\beta_-{-}q^2}{\beta_-{}^2}J_{00}{}^+\Bigg],\end{aligned}$$

$$F_6{}^+=\left[\frac{1}{\beta_-}\ln\left|\frac{Q^2}{\beta_+}\right|+\frac{q^2}{\beta_-(\beta_+{+}\beta_-)}\ln\left|\frac{Q^2}{q^2}\right|-\frac{Q^2}{\beta_-{}^2}J_{00}{}^+\right],$$

$$F_7{}^+=\left[-\frac{2\beta_-{+}2Q^2}{Q^2\beta_-{}^2}\ln\left|\frac{Q^2}{\beta_+}\right|+\frac{1}{\beta_-(\beta_+{+}\beta_-)}+\frac{\beta_-{+}2Q^2}{\beta_-{}^3}J_{00}{}^+-\frac{q^2(5Q^2\beta_-{+}2Q^2\beta_+{-}2q^2\beta_-)}{\beta_-{}^2Q^2(\beta_+{+}\beta_-)^2}\ln\left|\frac{Q^2}{q^2}\right|\right],$$

$$F_8^+=\left[\frac{q^2}{\beta_+(\beta_++\beta_-)^2}\ln\left|\frac{Q^2}{q^2}\right|-\frac{1}{\beta_+(\beta_++\beta_-)}\right],$$

$$F_9^+=\left[-\frac{Q^2+2\beta_-}{Q^2\beta_-(\beta_++q^2)}\ln\left|\frac{Q^2}{\beta_+}\right|-\frac{1}{\beta_+(\beta_++\beta_-)}+\frac{1}{\beta_-^2}J_{00}^+ +\left(\frac{q^2}{\beta_+(\beta_++\beta_-)^2}-\frac{q^2}{\beta_+\beta_-(\beta_++q^2)}-\frac{2q^2(Q^2+\beta_+)}{Q^2\beta_+(\beta_++\beta_-)(\beta_++q^2)}\right)\ln\left|\frac{Q^2}{q^2}\right|\right],$$

$$F_{10}^+=\left[\frac{q^2(\beta_--2\beta_+-2q^2)}{\beta_-^2(\beta_++q^2)^2}\ln\left|\frac{Q^2}{\beta_+}\right|+\frac{2q^2}{\beta_-^3}J_{00}^++\frac{q^2-\beta_-}{\beta_-(\beta_++\beta_-)(\beta_++q^2)}+\left(\frac{q^2(2\beta_+-\beta_-+2q^2)}{\beta_-^2(\beta_++q^2)^2}-\frac{q^2(2\beta_++3\beta_-)}{\beta_-^2(\beta_++\beta_-)^2}\right)\ln\left|\frac{Q^2}{q^2}\right|\right],$$

$$F_n^-=F_n^+(p_+\leftrightarrow p_-),$$

where

$$J_{00}^+=\tfrac{1}{2}\ln^2\left|\frac{Q^2}{\beta_+}\right|+\tfrac{1}{2}\pi^2\theta(-Q^2)-\tfrac{1}{2}\pi^2\theta(-\beta_+)+g+f^+,$$

$$g=\left[\ln\left|\frac{Q^2-q^2}{Q^2}\right|\ln\left|\frac{Q^2}{q^2}\right|+\tfrac{1}{2}\ln^2\left|\frac{Q^2-q^2}{Q^2}\right|-\tfrac{1}{2}\pi^2\theta\left(\frac{Q^2q^2}{Q^2-q^2}\right)-L\left(\frac{q^2}{Q^2-q^2}\right)-\tfrac{1}{12}\pi^2\right],$$

$$f^+=\left[-\ln\left|\frac{q^2}{\beta_+}\right|\ln\left|\frac{\beta_++q^2}{\beta_+}\right|+L\left(\frac{q^2}{\beta_+}\right)+\tfrac{1}{12}\pi^2\right],$$

($g\to 0$ as $q^2/Q^2\to 0$ and $f^+\to 0$ as $q^2/\beta_+\to 0$),

$$L(x)=\mathrm{Re}\left\{\int_1^x\frac{\ln(1+y)}{y}dy\right\},$$

$$L(x)=-\tfrac{1}{12}\pi^2+\left(x-\frac{x^2}{2^2}+\frac{x^3}{3^3}-\cdots\right),\quad x<1$$

$$L(x)=\tfrac{1}{2}\ln^2|x|-\tfrac{1}{2}\pi^2\theta(-x)-L(1/x),\quad x>1$$

$$L(-1)=-\tfrac{1}{4}\pi^2\quad\text{(see Ref. 21)},$$

$$H_0(Q^2)=\frac{-iQ^2}{\pi^2}\int\frac{d^4l}{(l^2-\lambda^2)(l^2+2p_+\cdot l)(l^2-2p_-\cdot l)},$$

$$\theta(x)=1,\quad x>0;\qquad =0,\quad x<0.$$

$H_0+\ln(\lambda^2/m^2)$ contains the infrared divergence. The term cancels identically against a similar term in the soft-photon correction (see Sec. III B). Most of the virtual photon correction is contained in the "multiplicative" term of Eq. (B1), namely, the first term where the radiative correction is proportional to the Bethe-Heitler matrix element.

1. Bremsstrahlung

Bremsstrahlung is connected to pair production by the transformation $k\to -k'$, $p_+\to -p_{\text{in}}$, and $p_-\to p_{\text{out}}$, where p_{in} is the incoming electron in bremsstrahlung, p_{out} is the scattered electron, and k' is the emitted photon. Specializing to low momentum transfers and to the experimental situation where p_{out} and k' are emitted nearly symmetrically (defined as $2p_{\text{in}}\cdot p_{\text{out}}\cong 2p_{\text{in}}\cdot k'\cong p_{\text{out}}\cdot k'$), the result is

$$d\sigma_{\text{BR}}{}^{\text{vir}}=\frac{\alpha}{2\pi}\left[-2H_0(-2p_{\text{in}}\cdot p_{\text{out}})-2\ln\frac{\lambda^2}{m^2}+3\ln\frac{2k'\cdot p_{\text{in}}}{m^2}+\tfrac{4}{3}\ln\left|\frac{q^2}{m^2}\right|-\frac{65}{9}+\tfrac{1}{2}\pi^2+\tfrac{3}{2}\ln 2+\tfrac{1}{2}(\ln 2)^2+\left(-\frac{1}{5}\frac{\pi^2}{2}+\tfrac{1}{2}(\ln 2)^2+\frac{17}{10}\ln 2+\frac{1}{5}\right)\right]d\sigma_{\text{BR}}.\quad\text{(B2)}$$

The term in parentheses comes from the nonmultiplicative terms of Eq. (B1) which becomes multiplicative near symmetry because of the dip. However, we

have ignored one term which even near symmetry is nonmultiplicative. It is less than $(18/5)(\alpha/2\pi)d\sigma_{BR}$. The infrared divergent terms cancel against the soft-photon correction which, together with the hard-photon correction, may be calculated by applying the above transformation to the results for pair production.

2. Trident Production

The radiative correction to trident production contains diagrams like the ones in Fig. 2, except that the incoming photon is virtual. Equation (B1) is still useful, however, because we may make the transformation $k\leftrightarrow -q$ and interpret the result as the radiative correction to pair production by virtual photons but at low momentum transfers ($q^2\approx 0$). The errors inherent in calculating radiative corrections to trident production would seem to justify ignoring all but the first term of Eq. (B1).

APPENDIX C: APPROXIMATE HARD-PHOTON CORRECTION

Here we give an approximate expression for the hard-photon correction to symmetric pair production. The peaking approximation Eq. (3.11) is used as well as the expansion of $d\sigma_{BH}$ given in Eq. (1.7). We set

$$S(2E+l_0)\cong S(2E)2E/(2E+l_0)$$

and ignore the dependence of $G_E^2(q^2)$ on l_0. The result is

$$d\sigma_{BH}{}^{hard}\cong -\frac{\alpha}{\pi}\left(\ln\frac{Q^2}{m^2}-1\right)\left[\ln\frac{\delta^2}{(\Delta E)^2}d\sigma_{BH}+I(p_+,p_-,\Delta E)\right],$$

$$\begin{aligned}I(p_+,p_-,\Delta E)=d\sigma_{BH}&\left[\tfrac{1}{2}\ln\frac{(\Delta+v)^2+w^2}{v^2+w^2}+\tfrac{1}{2}\ln\frac{(\Delta'-v)^2+w^2}{v^2+w^2}+2\ln\frac{2E+\Delta E}{2E}\right]-d\sigma_{BH}(\text{sym})\tfrac{1}{4}\left\{\tfrac{13}{2}\ln\frac{(\Delta+v)^2+w^2}{v^2+w^2}\right.\\
&+\left(\frac{1}{(v+\Delta)^2+w^2}-\frac{1}{v^2+w^2}\right)\left[\frac{\theta^2}{8}\frac{1}{v^2+w^2}\left(\frac{v^2}{w^2}-1\right)+\frac{5}{1-\epsilon}\frac{\theta^2 v}{8w^2}\left(1+\frac{13}{5}v\right)+\frac{13}{2}\frac{\theta^2}{4}\right]\\
&+\left(\tan^{-1}\frac{\Delta+v}{w}-\tan^{-1}\frac{v}{w}\right)\left[\frac{v}{w^3}\frac{\theta^2}{8}\frac{1}{v^2+w^2}-\frac{v^2+\varphi^2/4}{(v^2+w^2)^2}\frac{v}{w}-\frac{5}{1-\epsilon}\left(\frac{\varphi^2}{2}+\frac{\theta^2}{4}\right)\frac{1}{2w^3}\left(1+\frac{13}{5}v\right)\right]\\
&\left.+\frac{\Delta}{(\Delta+v)^2+w^2}\left[\frac{\theta^2}{8}\frac{1}{v^2+w^2}\frac{v}{w^2}+\frac{5}{1-\epsilon}\frac{\theta^2}{8w^2}\left(1+\frac{13}{5}v\right)\right]+(\text{same with } v\to -v,\ \Delta\to\Delta',\ \epsilon\to -\epsilon)\right\},\end{aligned}\tag{C1}$$

where

$$v=(a+\epsilon);\qquad w^2=\tfrac{1}{4}\varphi^2+\tfrac{1}{4}\theta^2,$$

$$\Delta=\frac{\Delta E}{2E+\Delta E}(1-\epsilon);\quad \Delta'=\frac{\Delta E}{2E+\Delta E}(1+\epsilon).$$

See Fig. 6 for some graphs of this result.

APPENDIX D: THIN-TARGET CORRECTION

After the photon beam has interacted with the nuclei in the target to produce lepton pairs, it is possible for the real leptons to radiate on the way out of the target. Thus, for example, the experimental apparatus would accept the pair produced with momenta p_+ and p_-+l followed, at another point in the target, by the radiation from the electron of a photon of momentum l. The correction due to this effect is called the target correction and should not be confused with the real photon correction which results from the radiation of a photon at the interaction point. By a thin target we mean a target in which the probability of a lepton radiating twice is negligible. Thick-target corrections have been considered recently by Tsai and Whitis.[28]

Consider a lepton of energy E_0 interacting with a nucleus and radiating a photon of energy l_0. The probability of this happening in the target is in the Born approximation.[29] (See diagrams Fig. 5–7 and Fig. 5–8.)

$$dp(E_0,E)=\frac{dl_0}{l_0}\frac{E}{E_0}\left[(\Gamma_1-\Gamma_2)+\frac{1}{2}\frac{l_0^2}{EE_0}\Gamma_1\right],\tag{D1}$$

where $E_0=E+l_0$. Γ_1 and Γ_2 are functions characteristic of the target. They involve integrals over nuclear form factors including, in particular, the effect of screening. For ease of notation, we have also included here macroscopic effects such as the shape of the target and its density distribution. For the case of complete screening, $E_0E/ml_0\gg 137Z^{-1/3}$, Γ_1 and Γ_2 are independent of E_0 and E.

[28] Y. S. Tsai and Van Whitis, Phys. Rev. **149**, 1248 (1966).

[29] A. Sorenssen, Nuovo Cimento **38**, 745 (1965).

It is convenient to relate the functions Γ_1 and Γ_2 to the effective length of the target in radiation lengths. For the case of complete screening,

$$t_{\rm rad}^{\rm eff}=\frac{1}{E_0}\int_0^{E_0} l_0 dp(E_0,E)=\tfrac{1}{2}(\Gamma_1-\Gamma_2)+\tfrac{1}{6}\Gamma_1. \quad \text{(D2)}$$

To derive Eq. (D1) the angles of the photon and of the outgoing lepton have been integrated over. Nonetheless, we know that at high energies the photon is radiated dominantly in the direction of motion of either the incoming or the outgoing lepton. Furthermore, we know that bremsstrahlung is dominated by low momentum transfer events ($|q^2|\sim m^2$). We therefore make the high-energy approximation that the result of radiating in the target is to change the energy of the radiating particle but not its direction of motion. The cross section for producing a pair of leptons, one of which subsequently radiates, is then

$$\begin{aligned}d\sigma_{\rm BH}^{\rm target}=&\int_\delta^{l_0({\rm max}+)} d\sigma_{\rm BH}(E_++l_0,E_-)dp(E_++l_0,E_+)\\&+\int_\delta^{l_0({\rm max}-)} d\sigma_{\rm BH}(E_+,E_-+l_0)dp(E_-+l_0,E_-)\\=&\int_\delta^{l_0({\rm max}+)}\frac{dl_0}{l_0}d\sigma_{\rm BH}(E_++l_0,E_-)\frac{E_+}{E_++l_0}\\&\times\left[(\Gamma_1-\Gamma_2)+\frac{1}{2}\frac{l_0^2}{E_+(E_++l_0)}\Gamma_1\right]\\&+\int_\delta^{l_0({\rm max}-)}\frac{dl_0}{l_0}d\sigma_{\rm BH}(E_+,E_-+l_0)\frac{E_-}{E_-+l_0}\\&\times\left[(\Gamma_1-\Gamma_2)+\frac{1}{2}\frac{l_0^2}{E_-(E_-+l_0)}\Gamma_1\right]. \quad \text{(D3)}\end{aligned}$$

The integral diverges at $l_0=0$, but the divergence is cancelled by the contribution from the virtual correction to lepton-nuclear scattering without radiation. From our work in the body of this paper the result is clearly

$$d\bar\sigma_{\rm BH}^{\rm target}=(\Gamma_1-\Gamma_2)\ln\frac{\delta^2}{E_+E_-}+d\sigma_{\rm BH}^{\rm target}. \quad \text{(D4)}$$

The remainder of the soft-photon correction is negligible because the scattering is dominated by small momentum transfer events.

Equation (D4) is similar to Eq. (3.11). Thus one may think of the real photon correction in the peaking approximation as pair production followed by bremsstrahlung characterized by certain values of Γ_1 and Γ_2. The result is similar to the result of Lomon[12] but good in our formulation to all orders in l_0.

For symmetric pair production we can ignore the $\frac{1}{2}l_0^2/E_0E$ term in (D1). Using Heitler's[30] result that $\Gamma_2=\frac{1}{3}\Gamma_1$, we may rewrite Eq. (D4) as

$$\begin{aligned}d\bar\sigma_{\rm BH}^{\rm target}=&\tfrac{4}{3}t_{\rm rad}^{\rm eff}\left\{\ln\frac{\delta^2}{E_+E_-}\right.\\&+\int_0^{\Delta E}\frac{dl_0}{l_0}d\sigma_{\rm BH}(E_++l_0,E_-)\frac{E_+}{E_++l_0}\\&\left.+\int_0^{\Delta E}\frac{dl_0}{l_0}d\sigma_{\rm BH}(E_+,E_-+l_0)\frac{E_-}{E_-+l_0}\right\}, \quad \text{(D5)}\end{aligned}$$

where $\Delta E=k_{\rm max}-E_+-E_-$.

For a uniform, rectangular target

$$t_{\rm rad}^{\rm eff}=\tfrac{1}{2}t_{\rm rad}, \quad \text{(D6)}$$

where $t_{\rm rad}$ is the thickness of the target in radiation lengths. The real photon correction to symmetric pair production may be thought of simply as a target correction with

$$t_{\rm rad}^{\rm eff}=\frac{3}{4}\frac{\alpha}{\pi}\left(\ln\frac{Q^2}{m^2}-1\right). \quad \text{(D7)}$$

[30] W. Heitler, *The Quantum Theory of Radiation* (Oxford University Press, London, 1954), Chap. V, p. 25.